Regulation of spatially developing free shear flow in steady desired state by closed-loop control

Diemer Anda Ondo, Johan Carlier, Christophe Collewet

Regulation of spatially developing free shear flow in steady desired state by closed-loop control

Diemer Anda Ondo and Johan Carlier
Irstea, UR TERE, F-35044 Rennes Cedex, France
Christophe Collewet
Irstea, UR TERE, F-35044 Rennes Cedex, France
Inria, Campus universitaire de Beaulieu, F-35042 Rennes Cedex, France

I. Introduction

Entrainment and mixing processes in the turbulent layer between two adjacent fluids are commonly involved in industrial applications. In case of a spatially developing plane shear layer, induced by two parallel incident streams with velocity and fluid differences, the flow is convectively unstable and a typical noise amplifier, leading to a very high sensitivity to upstream boundary conditions. Open- or closed-flow control by acting on its upstream conditions is therefore promising to enhance or reduce mixing due to turbulence.

Coherent structures of the turbulence in plane free shear layer can be view in many flow visualization experiments. It is shown in Ref. 1 and 2 that turbulence is conducted by large spanwize roller vortices surrounded by smaller quasi-streamwize rib vortices. Roller vortices come from the development of perturbation due to Kelvin-Helmholtz instability leading to vortex shedding at Strouhal frequency and near the inflection point of the velocity profile.[3,4] Rib vortices come from three-dimensional shear instabilities in the thin vortical braid region between the rollers.[5] Together with spanwise oscillations of rollers, they speed up the transition to fully three-dimensional turbulence.

Self similar behavior of the mixing layer occuring downstream to the transition region is inescapable. Self similar behavior means geometric affinity of the turbulence statistic profiles and linear growth of the mixing layer thickness. Nevertheless, upstream conditions influence the mixing layer development in the transition and the self-similar regions, as for example the length of the transition region and the constant spreading rate in the self-similar region.

Putting aside effects of velocity and density ratios between the two streams, many studies showed periodic excitations act significantly on the mixing layer development. They trigg the roller vortex shedding and therefore modify the structure of the flow in the mixing layer and its downstream evolution, at least in the transition region. Open-loop control was achieved in Ref. 6,7,8 using a predeterminated periodic excitations. Closed-loop control of the mixing layer, more robust and efficient due to the use of measures in the loop which allow to adapt and check the control, has been recently investigated in Ref. 9, 10, 11. In Ref. 9 and 10, a temporally developing mixing layer was used to make easier the design of a predeterminated control optimizing the thickness of the mixing layer, this predeterminated control being applied in open-loop on the spatially developing mixing layer. In Ref. 11, different closed-loop approaches (extremum-seeking adaptive control, POD mode feedback control, machine learning control) were achieved by finding the optimal frequency actuation online (rather than offline as previous studies using open-loop control) that enhanced turbulence in the mixing layer.

In the present study, we achieved a classical control scheme from control theory, i.e. state feedback by Linear-Quadratic Regulator (LQR), able to maintain mixing-layer in a desired state and to reject upstream perturbations. Note that we just considered here a steady desired state as a first step in the way to cope with an unsteady desired state as a particular space-time organization of the flow knowing the benefits for industrial applications. The paper is structured as follow. Section II is devoted to fluid flow modeling and

the closed-loop control design, including an original model reduction based on simple fluid flow assumption. Section III presents the behaviour of the linearized model and the control law applied to a Navier-Stokes 3D solver. The ability of the control law to reject disturbances is also discussed.

II. Control design

II.A. Governing equations

In incompressible flow and Newtonian fluid, the motion of viscous fluid is described by the Navier-Stokes equations

$$\left\{ \begin{array}{lcl} \partial_t \mathbf{u} + (\mathbf{u}\cdot\nabla)\mathbf{u} & = & -\frac{1}{\rho}\nabla p + \frac{1}{Re}\Delta \mathbf{u}, \\ \nabla\cdot\mathbf{u} & = & 0, \end{array} \right. \tag{1}$$

where $\mathbf{u}$ is the velocity field vector defined as $[u \quad v \quad w]^T$ and p the pressure, both being non-dimensionalized using the velocity difference between the two free stream $U_0 = U_2 - U_1$ and the initial thickness of the shear layer δ_0. In this system, the dynamic viscosity of the fluid appears as the Reynolds number $Re = \frac{U_0\delta_0}{\nu}$.

The flow was assumed to be near the desired profile $\mathbf{U}_b$ which corresponded to the steady $2D$ incompressible base-flow solution so that

$$\left\{ \begin{array}{lcl} (\mathbf{U}_b\cdot\nabla)\mathbf{U}_b & = & -\frac{1}{\rho}\nabla p + \frac{1}{Re}\Delta \mathbf{U}_b, \\ \nabla\cdot\mathbf{U}_b & = & 0. \end{array} \right. \tag{2}$$

In this study, the Blasius solution of this system with free shear layer boundary conditions was approximed by

$$\mathbf{U}_b = \left[U_1 + \frac{1}{2}\left(\tanh(y-y_0)+1\right), \quad 0, \quad 0 \right]^T. \tag{3}$$

It is of note that this desired profile is homogeneous in the streamwise direction x, and then does not take into account the slight physical extension of the shear layer downstream. For the given profile $\mathbf{U}_b = [U_b \quad 0 \quad 0]^T$ disturbed by $\mathbf{u'} = [u' \quad v' \quad w']^T$ and p' with $\mathbf{u'} \ll \mathbf{U}_b$, the Navier-Stokes equations (1) become

$$\left\{ \begin{array}{lcl} \partial_t u' + U_b\partial_x u' + v'\partial_y U_b & = & -\partial_x p' + \frac{1}{Re}\Delta u', \\ \partial_t v' + U_b\partial_x v' & = & -\partial_y p' + \frac{1}{Re}\Delta v', \\ \partial_t w' + U_b\partial_x w' & = & -\partial_z p' + \frac{1}{Re}\Delta w', \\ \partial_x u' + \partial_y v' + \partial_z w' & = & 0. \end{array} \right. \tag{4}$$

The state space model obtained from equations (4) leads to a descriptor system (due to the presence of the pressure p in the equations). Even there exists a considerable study on descriptor systems, we chose to determinate a standard linear system using vorticity-stream function formulation, see Ref. 12, 13. The stream function $\psi(x,y,t)$ is defined with $2D$ and incompressible flow hypothesis such that

$$u = \partial_y \psi \tag{5}$$

$$v = -\partial_x \psi \tag{6}$$

$$\omega_z = -\nabla^2 \psi, \tag{7}$$

where ω_z is the vorticity in spanwise direction z. This formulation allows to eliminate the pressure in the equations and will allow to design a standard state space model. The vorticity-stream function formulation is given by

$$\left[(\partial_t + U_b\partial_x)\Delta - U_b^{''}\partial_x - \frac{1}{Re}\Delta^2 \right]\psi = 0. \tag{8}$$

where $U_b^{''}(y)$ is the second derivative of $U_b(y)$ with respect to y. It is of note that plane wave perturbation leads eq. (8) to the well-know Rayleigh or Orr-Sommerfeld equations.[12]

II.B. Boundary conditions

The extent of the considered domain was $L_x \times L_y = 64 \times 16$. Dirichlet boundary conditions are used at the top and bottom boundaries with

$$\mathbf{u'}\left(x, y - y_0 = \pm 8, t\right) = 0. \tag{9}$$

Input and output boundaries were defined separately. The output boundary was used to preserve the continuity at $x = 64$, so that

$$\partial_x \mathbf{u'}\left(x = 64, y, t\right) = 0. \tag{10}$$

and the input boundary was modeled to take in account the control. The input boundary can be modeled as a function $\chi\left(x, y, t\right)$ to take into account the overall effect of downstream actuators (jet, plasma, wind blower...). Without loss of generality, this function was decomposed as a separable function such that

$$\chi(x, y, t) = f(x)\Omega(y)\Gamma(t), \tag{11}$$

where

- $f\left(x\right)$ represents the effects of the input control in streamwise direction and is defined such that

$$\begin{aligned} \text{for } x = 0, \quad \chi &= \Omega(y)\Gamma(t), && \text{(12a)} \\ \text{for } x = 0, \quad \partial_x\chi &= 0, && \text{(12b)} \\ \text{for } x = 64, \quad \chi &= 0, && \text{(12c)} \\ \text{for } x = 64, \quad \partial_x\chi &= 0. && \text{(12d)} \end{aligned}$$

  These conditions lead to the function $f(x) = 2(\frac{x}{64})^3 - 3(\frac{x}{64})^2 + 1$, see Ref. 13;

- $\Omega\left(y\right)$ represents the control of two wind blowers used to get the two co-flowing streams U_1 and U_2. Comparing to the literature (see Ref. 3), $\Omega(y)$ is often given by

$$\Lambda \exp^{-\sigma|y-y_0|}. \tag{13}$$

  In this study, we kept $\frac{U_1+U_2}{2}$ constant so that we chose

$$\Omega\left(y\right) = \tanh(y - y_0);$$

- $\Gamma\left(t\right)$ represents the amplitude of the control.

Taking into account the input boundary, we converted the homogeneous equation (8) with unhomogeneous conditions (eq. in streamwise direction) into an unhomogeneous system with homogeneous conditions, see Ref. 13, 14, 15. For this purpose, the stream function was broken down into

$$\psi = \psi_h + \chi, \tag{14}$$

with χ the change applied at the boundary and ψ_h the corresponding inside stream function. Substituting ψ in the linearized Navier-Stokes equation (8), this equation becomes

$$\begin{cases} F(\psi_h) &= -F(\chi), \\ \psi_h(x = 0, y, t) &= 0, \\ \psi(x, y = \pm 1) &= 0, \end{cases} \tag{15}$$

where $F(\psi)$ is the left side of eq. (8).

II.C. Model reduction

The model we propose in this paper is obtained in two steps:

- a spacial discretization (in x and y directions) of the linearized Navier-Stokes equation (8) using a finite differences scheme to obtain a finite model. We used n_x and n_y as the number of discretized sites in x and y direction, respectively;

- an extraction of the equation in y_0 (centerline of the shear layer).

Applying the finite differences scheme to (15) (simply a 2nd-order centred scheme in this study) and taking into account the input boundary, we got a reduced system

$$\mathbf{A}_1\partial_t X_r + \mathbf{A}_2 X_r = \mathbf{B}_1\partial_t\Gamma(t) + \mathbf{B}_2\Gamma(t). \tag{16}$$

where X_r is the discretized ψ_h and corresponds to the state vector of dimension n_{xy}, $\mathbf{A}_1$ and $\mathbf{A}_2$ are matrices of dimension $n_{xy} \times n_{xy}$, $\mathbf{B}_1$ and $\mathbf{B}_2$ are matrices of dimension $n_{xy} \times 1$ and $n_{xy} = n_x \cdot n_y$ is the total number of discretized sites.

The matrix $\mathbf{A}_1$ is not singular, so that the eq. (16) is rewriten such that

$$\partial_t X_r = -\mathbf{A}_1^{-1}\mathbf{A}_2 X_r + \mathbf{A}_1^{-1}\mathbf{B}_1\partial_t\Gamma + \mathbf{B}_2\Gamma. \tag{17}$$

As the dynamic occuring at centerline of the shear layer lead and express the behavior of the overall shear layer, we extracted the n_x rows corresponding to the dynamic in y_0 ($y_{(1-n_y)/2} = -8$ and $y_{(n_y-1)/2} = 8$), so we can write

$$\partial_t X_0 = \sum_{i=(1-n_y)/2}^{(n_y-1)/2} \mathbf{A}_{0i} X_i + \mathbf{B}_{01}\partial_t\Gamma + \mathbf{B}_{02}\Gamma \tag{18}$$

where X_i is the discretized ψ_h in y_i. Matrices $\mathbf{A}_{0i}$, $\mathbf{B}_{01}$ and $\mathbf{B}_{02}$ allow to capture the effects of X_i, $\partial_t\Gamma$ and Γ, respectively, on the dynamic of X_0. X_i need to be expressed as function of X_0 to close the system. This was done using a numerical computation of eq. (17) under `Matlab2012` with Γ a sinusoidal function with a subharmonic. The scenario consisted to excitate the system with Γ and to measure the nodes in normal direction (the effects on streamwise direction are less important) the mean profile can be obtained for a given time. This obtained mean profile could be approximated using a Gaussian function such that

$$X_i = e^{-d(y_i-y_0)^2} X_0, \tag{19}$$

with $d \simeq 1/(2 * 0.119)$.

Using eq. (18) and eq. (19), we can define a reduced controlled state space model given by

$$\partial_t X(t) = \mathbf{A}X(t) + \mathbf{B}\mathbf{q}(t), \tag{20}$$

with the control vector $\mathbf{q} = \partial_t\Gamma$, the considered state vector $X = \begin{bmatrix} X_0^T & \Gamma^T \end{bmatrix}^T$ and dynamic and control matrices are

$$\mathbf{A} = \begin{bmatrix} \sum_{i=(1-n_y)/2}^{(n_y-1)/2} \mathbf{A}_{0i} e^{-d(y_i-y_0)^2} & \mathbf{B}_{02} \\ 0 & 0 \end{bmatrix} \tag{21}$$

and

$$\mathbf{B} = \begin{bmatrix} \mathbf{B}_{01} \\ 1 \end{bmatrix}. \tag{22}$$

The properties of this linearized state is discussed in section III.

II.D. Control law

Let consider the system (20), we want to design a linear quadratic control law and therefore consider the following cost function to minimize

$$J = \int_0^\infty (X^T(t)\mathcal{Q}X(t) + \mathbf{q}^T(t)\mathcal{R}\mathbf{q}(t))\mathrm{dt} \tag{23}$$

where $\mathcal{Q}$, a semi-definite positive matrix ($\mathcal{Q} = \mathcal{Q}^T \geq 0$), and $\mathcal{R}$, a definite positive matrix ($\mathcal{R} = \mathcal{R}^T > 0$), are weighted matrices.

It is of note that the cost function was based on the the full state space, as in Ref. 16, 17. Indeed, the use of image sensor in fluid mechanic enables the measure in an efficient way of the flow state, see Ref. 18.

The control is computed using a feedback gain such that

$$\mathbf{q} = -\mathbf{K}X \tag{24}$$

with $\mathbf{K} = \mathcal{R}^{-1}\mathbf{B}^T\mathcal{P}$ and $\mathcal{P}$ is the solution of the well known algebraic Riccati equation

$$\mathbf{A}^T\mathcal{P} + \mathcal{P}\mathbf{A} - \mathcal{P}\mathbf{B}\mathcal{R}^{-1}\mathbf{B}^T\mathcal{P} + \mathcal{Q} = 0. \tag{25}$$

The weighted matrices $\mathcal{Q}$ and $\mathcal{R}$ are chosen to ensure a correct behavior of the closed-loop system. The matrix $\mathcal{Q}$ is such that $X^T\mathcal{Q}X$ is related to the turbulent kinetic energy of the system, see Ref. 13. The matrix $\mathcal{R}$ was chosen such that $\mathcal{R} = r^2\mathbb{I}$ where r was adjusted depending on the ability of the designed control law to lead the system through the desired profile on the linearized system. In our case, $\mathbb{I} = 1$ as we have a scalar control ($\mathbf{q}$).

III. Results

In this section, we discuss the characterization of the linearized state space model derived from the navier-Stokes equations and the obtained results on `Incompact3D` with the control law eq. (24) obtained from the state space model.

III.A. Behavior of the state space model

The search of a control for the mixing layer assumes that the system is controllable, that means there exists a control $\mathbf{q}$ such that the solution $X(t) \to X_f$ when $t \to t_f$. Using the Popov-Belevitch-Hautus (PBH) criteria, see,[19] it can be seen that the state space model is stabilizable.

In the particular case of the linearized system about a desired state, it's obvious that the stabilizability will be equivalent to the controllability if the final state is the desired profile (despite the numerical problem which can be encountered from sparse matrices). We note also that the state space model $\mathbf{A}$ is stable as expected for a noise amplifier flow. Indeed, all its eigenvalues lie in the left half complexe plane except one which is null, but their real part are very closed of the imaginary axis. The objective of our proposed control law in (24) will be to improve the stability of the closed-loop system such that we ensure the minimal kinetic energy in the system whatever disturbances are.

The stability of the state space means that in the absence of permanent disturbance, the system will converge to the desired profile $\mathbf{U}_b$. In the next, we look at what happens if there is permanent disturbance to its input boundary. We consider the system given by

$$\partial_t X(t) = \mathbf{A}X(t) + \mathbf{B}\mathbf{q}(t) + \mathbf{B}\mathbf{w}(t), \tag{26}$$

where $\mathbf{w}(t)$ is the disturbance to be rejected and we assumed that disturbances and control acted on the system in the same way. We consider that $\mathbf{w}$ perturbs velocities U_1 and U_2 and we use the control law to compensate the effect of the disturbances. In that configuration, the disturbance acted on the input boundary and was seen as a perturbation on the control. The disturbances $\mathbf{w}(t)$ was formulated as a temporal sinusoidal excitation (to model fluctuations of the blowers) and was given by

$$\mathbf{w}(t) = \sum_{k=0}^{1} a_k \sin(2\pi f_k t), \tag{27}$$

where f_0 is the fundamental frequency (most amplified periodic perturbation, see[3]) and f_1 corresponds to its subharmonic ($f_1 = \frac{f_0}{2}$), $a_0 = 5e-3$ and $a_1 = \frac{a_0}{2}$.

We present on Fig. 1, the evolution of the input of the system (control law and disturbance) and the norm of the state vector in presence of the disturbances, with and without control. As can be seen, even if the system without control is stable, the flow is perturbated by the disturbance. The effects of this disturbance is far much lower when using our closed loop control scheme. Indeed, we remark that the obtained control was very closed to the opposite of the applied disturbance.

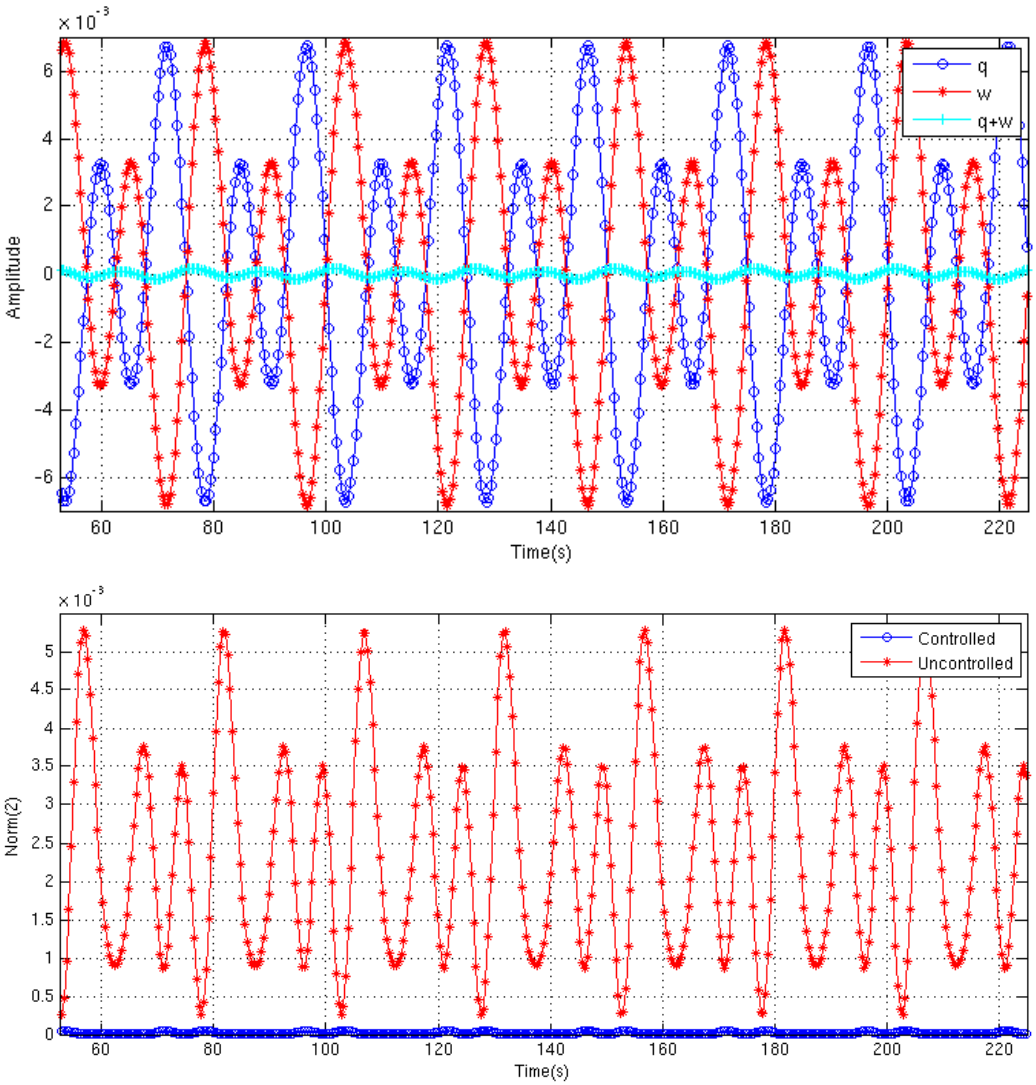

Figure 1. Evolution of the system: on top, the control law and the disturbance; on bottom the norm of the state vector in presence of permanent disturbances.

III.B. Behavior on the nonlinear model

To completely validated our control law we have now to apply it on the system obtained from the resolution of the 3D Navier-Stokes equations. This is done thanks to `Incompact3D` solver, see[20,21]

First, let us exam the behavior of the system without control and considering a perturbation $\mathbf{w}(t)$ described by (27) with $a_0 = 5e-3$ and $f_0 = 0.08$. We represent on Fig. 2 the vorticity map. As can be seen we observe the classical Kelvin-Helmholtz instabilities and pairing due to subharmonics. On the top, we represent the region of interest.The behavior we can expect from a classical excitation in terms of properties of the system (Kelvin Helmholtz instabilities, pairing due to subharmonic, ...) is exactly the one we obtained with our excitation. The idea here was to verify that whatever the configuration or the excitation/disturbances we encountered, we could lead the system to the desired profile.

We have to mention that we did not measure the whole system, but only data for $y = 128$ (corresponds to the center of the) in the region of interest. The considered measure was done using the number of considered sites in the linearized model ($n_x = 17$).

In this simulation and the one before, we started from the same saved configuration (simulation used to avoid difference induced by numerical initialization). The simulation proceeded such that the control was first applied alone (approximately for $3s$) and the disturbance was applied when it reached 0 (near $58s$ in global time).

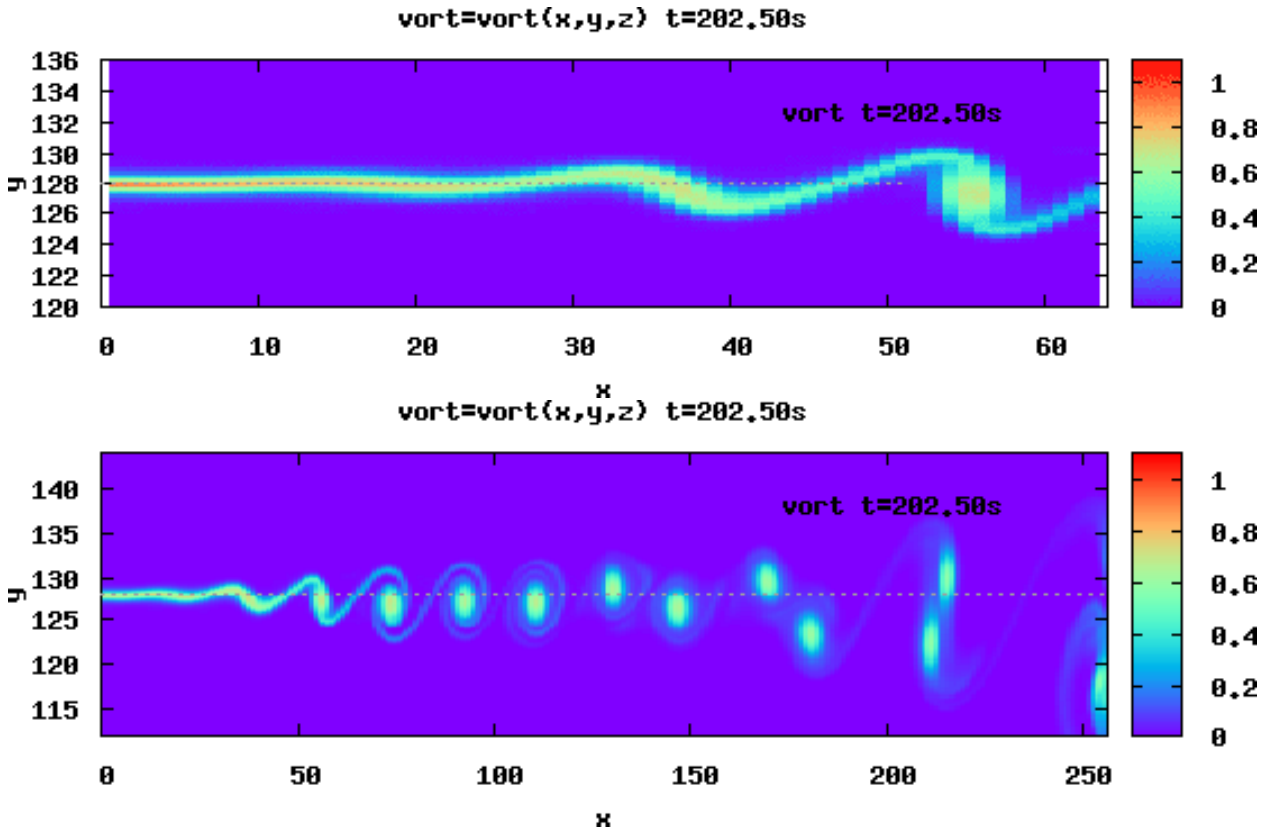

Figure 2. Instantaneous vorticity maps in the model plant in presence of permanent disturbances and without control after $202s$ of simulation: on top, a zoom on the region of interest; on bottom, the whole map.

We can see on Fig. 3 the effect of the proposed control law when the flow is perturbated by $\mathbf{w}(t)$ according to (27). The reject of the disturbance is estimated to more than 95% excepted for some periods where we just observed a rejection of 74% (the minimal rejection obtained near $184s$).

Fig. 4 depicts the vorticity map. Since the control law compensates the disturbance (see Fig. 3) the observation of the first Kelvin-Helmholtz instabilities is delayed. Moreover, as can be seen, the control law avoids the pairing of vortices and even avoids the construction of vortices in the region of interest. Fig. 4 has directly to be compared with Fig. 2.

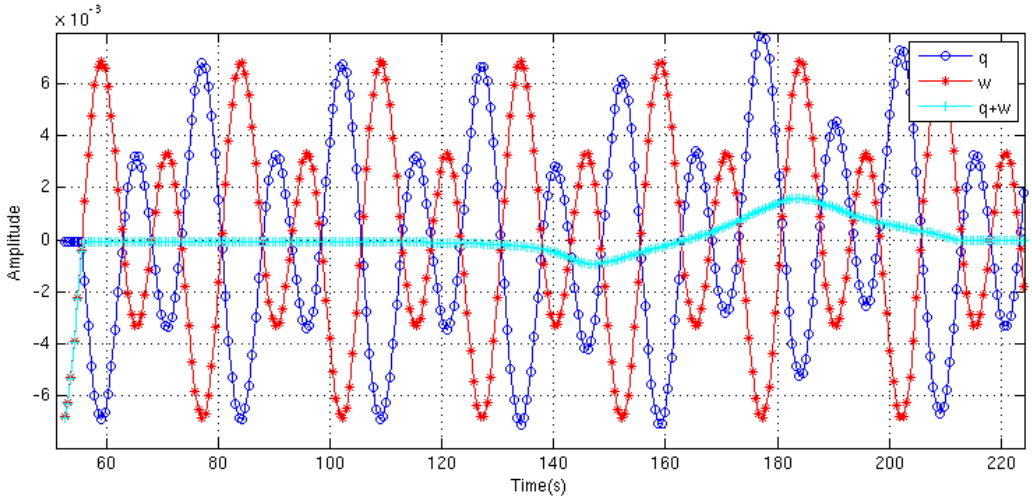

Figure 3. The evolution of the control in presence of permanent disturbances.

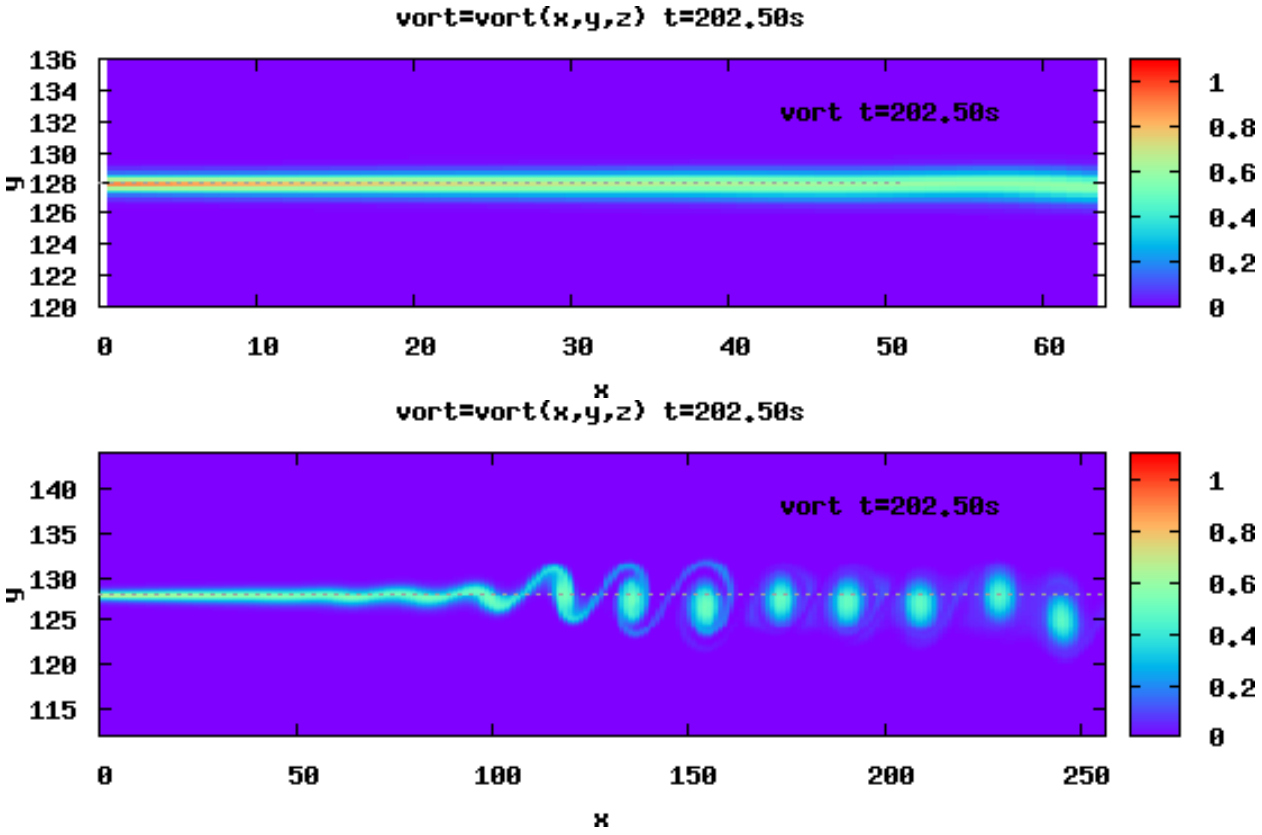

Figure 4. Instataneous vorticity maps in the model plant in presence of permanent disturbances and with control after $202.5s$ **of simulation: on top a zoom on the region of interest and on bottom the whole map.**

IV. Conclusion

In this paper, we showed the ability of feedback control to regulate spatially developing mixing-layer flow around a steady desired state, and to reject relatively slow disturbances compared to the acquisition rate. This was performed using a linear control law designed from a reduced linearized state space model of the Navier-Stokes equations. The reduction was based on basic assumption allowing to deal with the dynamic of the mixing layer only on the centerline. As the measure for the control loop are distributed along the centerline of the mixing layer, non-intrusive measurements method have to be used to prevent additional disturbances and wake effects on downstream measures. Optical method such as particule image velocimetry or optical flow are very appropriate, particularly if the analysis is restricted to a limited number of lines in the image. Further works will concern the case of an unsteady desired state and the validation on experiments in a dedicated wind tunnel, see Ref. 22.

References

[1]Brown, G. L. and Roshko, A., "On density effects and large structure in turbulent mixing layers," *J. Fluid Mech.*, Vol. 64, No. 4, 1974, pp. 775–816.

[2]Bernal, L. P. and Roshko, A., "Streamwise vortex structure in plane mixing layers," *J. Fluid Mech.*, Vol. 170, 1986, pp. 499–525.

[3]Michalke, A., "On spatially growing disturbances in an inviscid shear layer," *J. Fluid Mech.*, Vol. 23, 1965, pp. 521–544.

[4]Monkewitz, P. A. and Huerre, P., "Influence of the velocity ratio on the spatial instability of mixing layers," *Physics of Fluids*, Vol. 25, No. 7, 1982, pp. 1137–1143.

[5]Corcos, G. M. and Lin, S. J., "The mixing layer: deterministic models of a turbulent flow. Part 2. The origin of the three-dimensional motion," *J. Fluid Mech.*, Vol. 139, 2 1984, pp. 67–95.

[6]Oster, D., Wygnanski, I., Dziomba, B., and Fiedler, H., "On the effect of initial conditions on the two dimensional turbulent mixing layer," *Structure and Mechanisms of Turbulence I*, edited by H. Fiedler, Vol. 75 of *Lecture Notes in Physics*, Springer Berlin Heidelberg, 1978, pp. 48–64.

[7]Inoue, O., "Double-frequency forcing on spatially growing mixing layers," *J. Fluid Mech.*, Vol. 234, 1 1992, pp. 553–581.

[8]de Zhou, M. and Wygnanski, I., "The response of a mixing layer formed between parallel streams to a concomitant excitation at two frequencies," *J. Fluid Mech.*, Vol. 441, 8 2001, pp. 139–168.

[9]Kaul, U. K., *An Efficient CFD-based PID Control of Free Shear Layer Flow*, American Institute of Aeronautics and Astronautics, 2013.

[10]Kaul, U. K., *First Principles Based PID Control of Mixing Layer: Role of Inflow Perturbation Spectrum*, American Institute of Aeronautics and Astronautics, 2014.

[11]Parezanović, V., Laurentie, J.-C., Fourment, C., Delville, J., Bonnet, J.-P., Spohn, A., Duriez, T., Cordier, L., Noack, B. R., Abel, M., Segond, M., Shaqarin, T., and Brunton, S. L., "Mixing Layer Manipulation Experiment," *Flow, Turbulence and Combustion*, Vol. 94, No. 1, 2015, pp. 155–173.

[12]Schmid, P. J. and Henningson, D. S., *Stability and transition in shear flows*, Vol. 142, Springer, 2001.

[13]McKernan, J., *Control of Plane Poiseuille Flow: A theoretical and Computationnal Investigation*, Ph.D. thesis, Cranfield University, School of Engineering, 2006.

[14]Joshi, S. S., Speyer, J. L., and Kim, J., "A systems theory approach to the feedback stabilization of infinitesimal and finite-amplitude disturbances in plane Poiseuille flow," *J. Fluid Mech.*, Vol. 332, 1997, pp. 157–184.

[15]Joshi, S. S., Speyer, J. L., and Kim, J., "Finite dimensional optimal control of Poiseuille flow," *J. Guidance, Control and Dynamics*, Vol. 22, No. 2, 1999, pp. 340–348.

[16]Tatsambon Fomena, R. and Collewet, C., "Fluid Flow Control: a Vision-Based Approach," *Int. Journal of Flow Control*, Vol. 3, No. 2, 2011, pp. 133–169.

[17]Gautier, N. and Aider, J.-L., "Feed-forward control of a perturbed backward-facing step flow," *J. Fluid Mech.*, Vol. 759, 2014, pp. 181–196.

[18]Tropea, C., Yarin, A. L., and Foss, J. F., *Springer Handbook of Experimental Fluid Mechanics*, Springer Berlin Heidelberg, 2007.

[19]Green, M. and Limebeer, D. J. N., *Linear Robust Control*, Prentice-Hall, Inc., 1995.

[20]Lamballais, E., Fortune, V., and Laizet, S., "Straightforward high-order numerical dissipation via the viscous term for Direct and Large Eddy Simulation," *J. Comput. Phys.*, Vol. 230, No. 9, 2011, pp. 3270–3275.

[21]Laizet, S. and Li, N., "Incompact3d: A powerful tool to tackle turbulence problems with up to $O(10^5)$ computational cores," *International Journal for Numerical Methods in Fluids*, Vol. 67, No. 11, 2011, pp. 1735–1757.

[22]Sodjavi, K. and Carlier, J., "Experimental study of thermal mixing layer using variable temperature hot-wire anemometry," *Experiments in Fluids*, Vol. 54, No. 10, 2013, pp. 1–19.